water

MDPI

Article

Estimation of Polder Retention Capacity Based on ASTER, SRTM and LIDAR DEMs: The Case of Majdany Polder (West Poland)

Zbigniew Walczak [1,*], Mariusz Sojka [2], Rafał Wróżyński [2] and Ireneusz Laks [1]

[1] Institute of Construction and Geoengineering, Poznan University of Life Sciences, 60-637 Poznań, Poland; laks.ireneusz@gmail.com

[2] Department of Land Improvement, Environmental Development and Geodesy, Poznan University of Life Sciences, 60-637 Poznań, Poland; masojka@up.poznan.pl (M.S.); rafwro@up.poznan.pl (R.W.)

* Correspondence: zbw@up.poznan.pl; Tel.:+48-061-846-6412

Academic Editor: Thilo Hofmann

Received: 1 March 2016; Accepted: 23 May 2016; Published: 28 May 2016

Abstract: This study compares four digital elevation models (DEMs), based on various data sources, to define polder retention capacities. Two commercial and two publically available, free of charge data sources were used. Commercial sources are DEMs based on aerial images and LIDAR (Light Detection and Ranging) data. Free data source DEMs generated are based on: SRTM (Shuttle Radar Topography Mission) and ASTER GDEM (ASTER Global Digital Elevation Model). In addition, the impact of the spatial resolution of the numerical terrain model on the calculated polder volume was evaluated. A DEM based on LIDAR data was used as the reference model and was supplemented with our own geodetic GPS (Global Positioning System) measurements. In flood modeling and management, including retention of river valleys and polders, it is necessary to properly estimate their capacity and the relation between capacity and water level. The study showed the impact of quantitative and qualitative data sources in determining the retention capacity of a polder.

Keywords: polder; DEM accuracy; LIDAR; SRTM; ASTER; TIN; volume of polder

1. Introduction

Digital elevation models (DEMs) are often used to estimate the capacities of natural flood valleys and polders, as well as flood threats [1–6]. The polders in Poland were created mainly in the valleys of the largest rivers: Vistula, Oder and Warta. These polders are an important factor influencing the transformation of a flood wave. During floods, polders are flooded in order to protect the cities that are located along the river [7–11]. The accurate estimation of the polder volume is of particular importance, and the water that is stored in its area correlates with the decreasing of the flood wave and the mitigation of the threat of embankment breaks. After the flood, water is drained from the polder back to the river via the weirs by means of gravitation or mechanically with pumps. Polders are often intersected by channels and ditches to ensure the gravitational drainage of the excess water. The restoration of proper water conditions in the polder areas is necessitated by the fact that, due to their fertile soil, they are often used for agricultural purposes. The appropriate and accurate modeling of a polder (e.g., its volume) is a precondition for the correct estimation of flow parameters in the case of flooding. Numerical terrain models like DEMs are very useful for modeling polders. The possible sources of these DEMs can be Interferometric Synthetic Aperture Radar (InSAR), like SRTM (Shuttle Radar Topography Mission) or ASTER (Advanced Spaceborne Thermal Emission and Reflection Radiometer), photogrammetric methods with space and aerial images, laser scanning using airborne Light Detection and Ranging (LiDAR), and classical geodetic GPS surveys. In many countries,

including Poland, LIDAR data are developed for medium-sized and large river basins. In the absence of access to high-resolution data (e.g., LIDAR data), DEMs based on ASTER [12–14] or SRTM [15–17] data can be used. Modeling of floodplains in the small scale in low-resolution, low-precision surface elevation data is hardly possible [15]. In this case, the accuracy of the resulting map depends too much on DEM uncertainties and errors both in the horizontal and vertical directions. It is also important, from an economic point of view, that ASTER and SRTM data are free of charge. The quality of data that are used to develop the numerical model is of particular importance in this case [12,18–24]. It often occurs that, despite possessing quite accurate landscape data, records of some crucial elements in terms of flood protection, such as embankments, are very scant [25]. DEMs should be complemented by data on river bathymetry in order to create an integrated model of a river [23,26].

The purpose of this study was to determine whether it is possible to use generally available, free and commercial numeric terrain models to define polder volumes. In the paper, numerical terrain models that were developed based on the following systems were analyzed: SRTM, ASTER and the commercial medium-resolution Airborne-DEM. The impact of the spatial resolution of the numerical terrain model on the calculated polder volume was also evaluated. A DEM based on LIDAR data that were supplemented with geodetic GPS measurements was used as the reference model.

2. Study Area

Majdany Polder (Figure 1) is located approximately 4 km south-west of the town of Koło on the right bank of the Warta River (from 439 + 900 to 444 + 400 km) in the Kolska Valley. The polder is situated in three municipalities of the Wielkopolskie region: Koło, Kościelec and Dąbie. It is surrounded by a system of embankments from the sides of the Ner and Warta Rivers, which are 2155 and 4155 m long, as well as from the Rgilewka River with a backwater embankment, which is 375 m long. The gentle slope toward Majdany village acts as a natural barrier. The embankment system was designed for summer floods with an overflow probability rate of 10%. The polder features two weirs, Majdany (located at 444 + 200 km of the Warta River) and Powiercie (located at 440 + 400 km of the Warta River), which automatically fill the polder with the water of the Warta. The drainage of water occurs primarily automatically via the weirs (mainly the one in Powiercie). However, when the polder water level is lower than the weir threshold, water is drained with a ditch system and by way of the Tralalka watercourse to the compensation reservoir, and further on to the Powiercie pump station, with an efficiency of Q = 1.4 $m^3 \cdot s^{-1}$. The purpose of the pump station is to drain the water of the Tralalka to the Rgilewka River. The facility is also fitted with a gravitational drain to direct the water from the compensation reservoir of Tralalka to the Rgilewka River in case the water level of the Rgilewka is lower than the polder water level.

The polder area is used only partially as meadows. The rest of the polder area is wasteland. A large portion of the polder is free of bushes and trees. Some bunches of bushes and trees appear mainly to the right embankment of the Warta. In the area of the backwater embankment of the Rgilewka and the Warta dyke, there are numerous oxbows that are filled with water. Willow trees are abundant in the cutoff area of Ner.

The Majdany polder is an element of the ECONET-PL network as a node area 19M [27], and is listed as a mainstay within the CORINE biotopes network. This area is also a bird mainstay on the European level-PL076 Middle Warta River Valley [28], especially for water birds.

In 2005, within the "Program for the Oder—2006", embankment modernization was carried out. The project goal was to prevent the Majdany polder from being flooded during the vegetation period and to ensure the effective drainage of flood water in the spring. This initiative also aimed to improve the technical condition of the embankment in order to mitigate the probability of dyke interruption during the flood within the vegetation period. The modernization of the embankments included the consolidation of the existing dyke, increasing the threshold and profiling the body. The threshold level was determined in accordance with the Decree of the Minister of Environmental Protection, Natural Resources and Forestry on 20 April 2007 regarding the technical conditions for the water engineering

facilities and their locations [29] and amounted to 0.5 m above the design water level at a probability rate of $p = 10\%$ (for Class IV buildings). In addition, the Powiercie weir was reconstructed, and its threshold ordinate was adjusted to synchronize its operation with the Majdany spillway (completed in 1998).

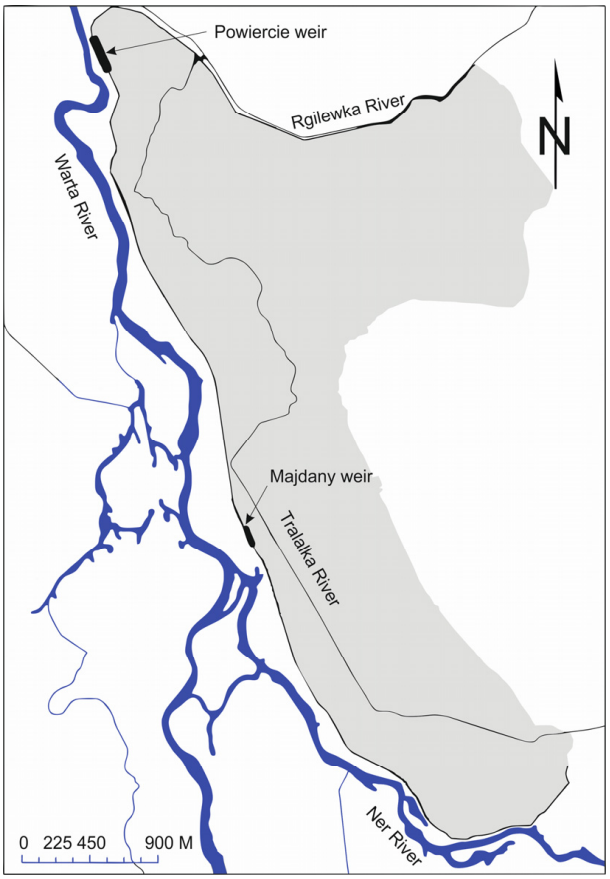

Figure 1. Study site location.

3. Methodology

In the course of this study, the following free and commonly available numerical terrain models were used: SRTM and ASTER GDEM V2.

In addition, two commercial DEMs were used: one from 2009, based on aerial images at the 1:26,000 scale, available in the TIN (Triangular Irregular Network) format, and LIDAR-DEM of 2011. A LIDAR-DEM was constructed based on data that were imported from aerial laser scanning within the IT System of the Country's Protection against Extreme Hazards (ISOK in Polish) 2011 [30], in sectional view 1:2500, available in the form of binary files in the LAS 1.2 format. The files were processed in order to filter out plants and buildings from the points cloud. File processing was performed with ArcGIS 10.0 software.

To estimate the accuracy of terrain and embankments modeling, our own terrain measurements were applied, performed with a GPS GRX-1 set by SOKKIA. The measurement accuracy of the applied device was 10 mm + 1 ppm for the X and Y coordinates and 20 mm + 1 ppm for the Z coordinate. More than 2000 measurements were performed, mainly of dykes. For communication and control purposes, Sokkia Spectrum Field ver. 8.1 was installed on controller SHC-250, as well as Topcon Link v.8 and Spectrum Survey Office v.8.2 for postprocessing purposes.

The numerical terrain model that was obtained with LIDAR data was quite accurate in terms of polder area modeling. The accuracy of dyke modeling and weirs for the LIDAR-DEM fluctuated from −0.33 m to 0.57 m [25]. The most frequent errors amounted to −0.1 m/0.1 and accounted for 85% of all

errors. The average square error RMSE (Table 1) of the embankments is 0.12 m, while the ME is 0.05 m, and the accidental error is SD 0.12 m (Table 2). The DEM based on aerial images (Airborne-DEM) was less accurate. Due to the above reasons, in this study, a LIDAR-DEM was used as the reference model, while the embankments were modeled based on our own measurements.

Table 1. Accuracy measures for embankments DEM.

Statistical Measures	
Average square error	$RMSE = \sqrt{\frac{1}{n}\sum_{i=1}^{n} h_i^2}$
Average error	$ME = \frac{1}{n}\sum_{i=1}^{n} h_i$
Accidental error	$SD = \sqrt{\frac{1}{(n-1)}\sum_{i=1}^{n} (h_i - ME)^2}$

Table 2. Result of Airborne-DEM and LIDAR-DEM embankment evaluations.

Error Indicator [1]	**Unit**	**Embankment**	
		Airborne-DEM	**LIDAR-DEM**
Min.	m	−1.86	−0.33
Max.	m	1.46	0.57
RMSE	m	0.72	0.12
SD	m	0.57	0.11
ME	m	−0.44	0.05

Note: [1] RMSE-average square error; ME—average error; SD—accidental error (see Table 1); Min and Max—the differences between the DEM and own terrain measurements with a GPS GRX-1.

The polder volume and area were calculated based on the numerical terrain models by means of ArcGIS 10.0 and the 3D Analyst and Area and Volume Statistics add-on. The polder volume was calculated as confined between 90.3 m above sea level (a.s.l.) and the embankment spillway threshold at 94.4 m a.s.l., for the LIDAR-DEM, ASTER-DEM, SRTM-DEM and Airborne-DEM models.

3.1. LIDAR Data

To date, analyses of flood area volumes most frequently have been related to numerical terrain models that were developed based on aerial (satellite) views, stereometry, data resulting from contour lines [5], and direct geodetic GPS measurements. Along with the ISOK system, numerical terrain models for the main river valleys of Poland are prepared based on LIDAR, which allows obtaining of a much more accurate DEM than before [5,10,25,31,32]. Its accuracy may depend on the land type (grassland, bushes and forests) [33]. One should also remember that raw LIDAR data require processing and therefore sometimes may cause significant problems [34]. This results mainly from the excessive amount of data, making it necessary to calculate the capacity and data filtering. Therefore, the resolution and LIDAR data density are often reduced (resampled), which may additionally affect the survey results [35]. Obviously, this density may also affect the quality of DEMs [36]. It is also sometimes necessary to filter out or remove medium and small flora, trees, or even buildings [37,38]. This removal naturally necessitates the application of appropriate filtering algorithms [39,40].

The LIDAR-DEM from the ISOK project [30] was used in this study. The point cloud covering the polder area included over 400 million points records (Figure 2).

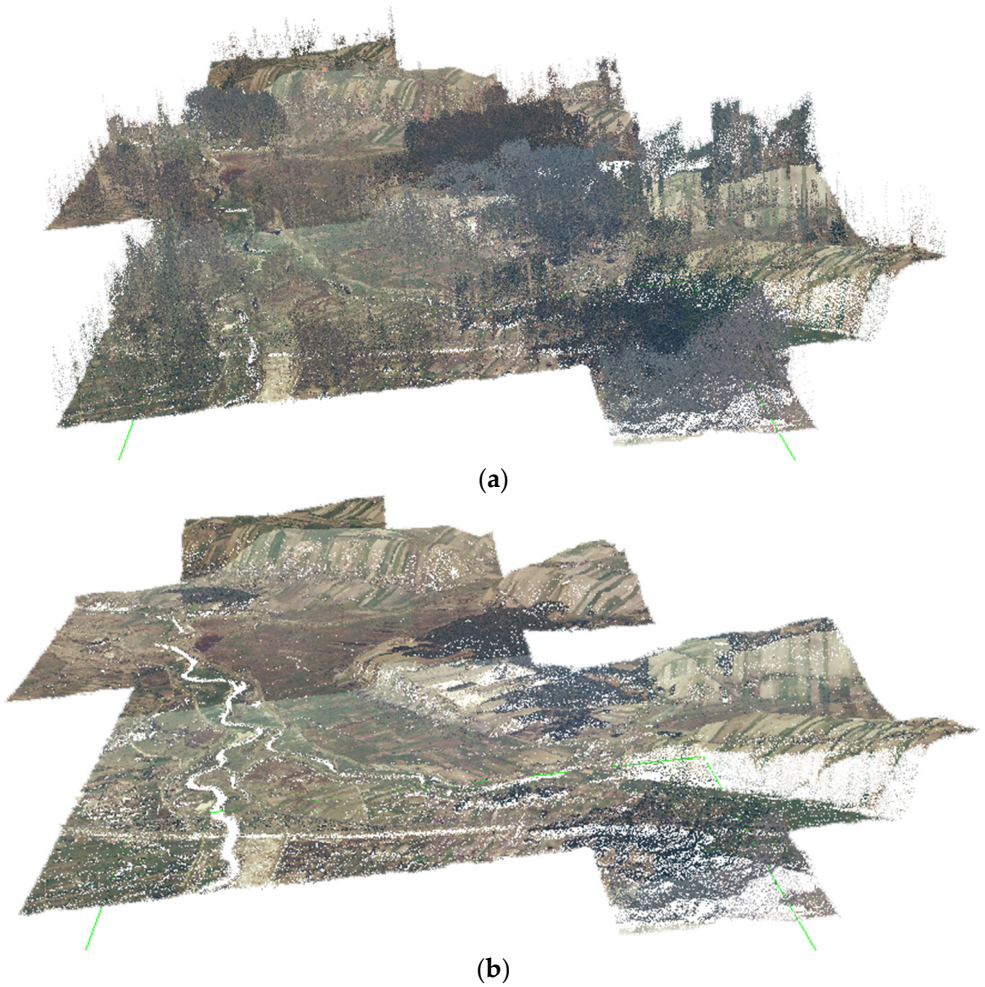

Figure 2. LIDAR point cloud (**a**) before and (**b**) after filtration.

Points with errors and small and medium flora and trees were filtered out (Figure 3).

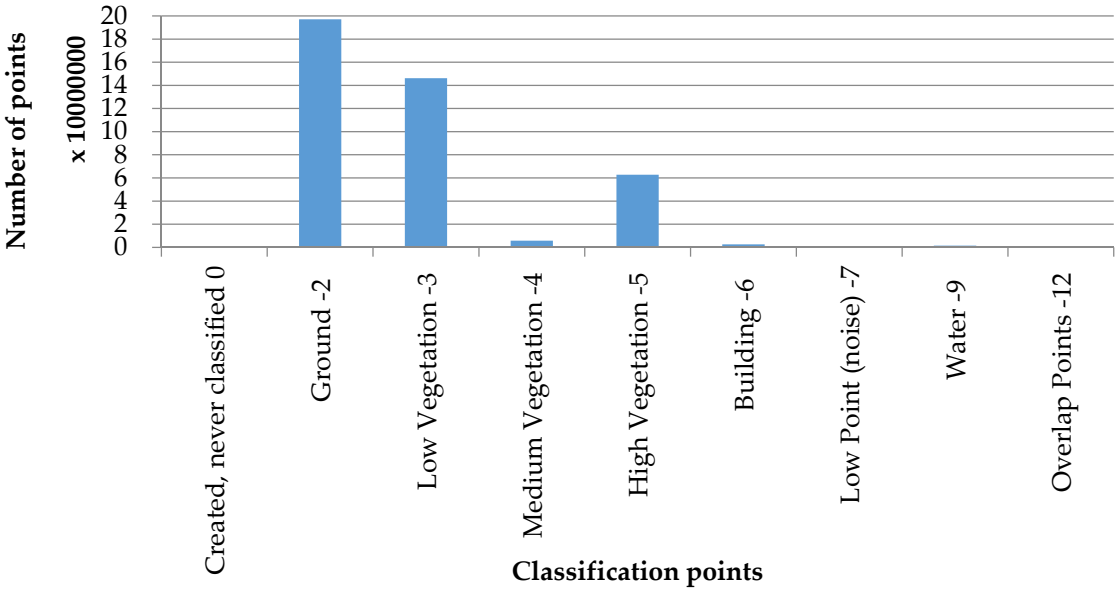

Figure 3. Point classification histogram.

Such a model was supplemented by field geodetic GPS measurements of embankments and spillways. As mentioned earlier, the model was used as a reference model for further analyses.

3.2. ASTER and SRTM Data

As an alternative for data obtained from aerial-view LIDAR, one may use The Shuttle Imaging Radar Mission (SRTM) [41] of 11 February 2000. This mission aimed at the interferometric reproduction of the topography of the entire Earth. The area of this mission covered almost 80% of the land between 60° North latitude and 56° South latitude. The data for the area of Poland are provided free of charge at a resolution of three seconds (90 m × 90 m); a higher resolution (30 m × 30 m) is available only in the USA. The following [42] tolerance values are assumed for the Eurasia zone: Absolute Geolocation Error of 8.8 m, Absolute Height Error of 6.2 m and Relative Height Error of 8.7 m. For the Wielkopolska region [43,44], it is assumed that the average measurement error is 3.7 m for a land inclination of 2° and 4.8 m for a land inclination of 2° to 6°. However, after eliminating the system error, the accuracy for the area of Poland is 1.0 m for plains and 2.7 m for hilly areas. This accuracy may vary, however, depending on the presence of vegetative cover plants [45]. As a rule, this accuracy is higher than that in the cartographic DEM [46].

Since 29 June 2009, as in the case of SRTM, data of the ASTER Global Digital Elevation Model have been provided free of charge [47]. For model generation, data that were collected by the ASTER scanner of the NASA (National Aeronautics and Space Administration) Terra satellite were used. The DEM, ASTER-DEM was established based on data that were collected 1999–2008, and it covers land between 83° North latitude and 83° South latitude at a grid resolution of 1 × 1 second (30 m × 30 m), which is theoretically higher than that of the SRTM data that are available in Poland. Since October 2011, the ASTER-GDEM is available in Model Version 2. The ASTER-GDEM V2 maintains the GeoTIFF format and the same gridding and tile structure as V1, with 30-meter postings and 1 × 1 degree tiles. The ASTER-GDEM V2 was used in this analysis.

The materials are available in the forms of both stereoscopic images and ready DEMs (free of charge). The accuracy of the ASTER-DEM oscillates around the elevation root-mean-square error (RMSE), which is 13 m–15 m, s less than the pixel size (15 m) [48–50]. The average errors of DEMs from ASTER stereoscopic images for flood areas reach just below 20 m [51]. Therefore, while comparing both free data sources, one can note that DEMs based on the SRTM mission (although with a worse resolution than that of ASTER) is more accurate and closer to the reference models [52–57]. DEMs may also be constructed as a combination of these two models [58] and, for example, OpenStreetMap [4].

ASTER-DEMs may be attractive, as these materials are available free of charge and for downloading directly from the web. The quality of data may be satisfying for various cartographic applications, however, discrepancies of even a few meters in practice exclude them for modeling flood zones.

Sometimes ASTER- and SRTM-DEMs could be useful for large-scale and regional models but inappropriate to local-scale ones. However both of these models require large statistical samples in order to determine their accuracy and to remove possible systematic error.

3.3. Airborne Data

Within the analysis, a DEM that was developed based on aerial images from 2009 was used at a scale of 1:26,000, available in TIN format (Airborne-DEM) consisting of dispersed altitude points forming a Triangulated Irregular Network. The specific files correspond to the section areas in the system of flat rectangular coordinates, 1992, scale 1:10,000.

According to the results [59], if the required accuracy is near 50 cm in the three directions, photogrammetry can be a useful 'fit-for-purpose' tool because the cost/gain and time/gain ratios are low. The photogrammetric DEM can been successfully used as input in a GIS-based hydrological and geotechnical model to derive sufficiently accurate slope and local drainage direction maps. Vertical

accuracy of the DEM is a function of photo scale and is estimated as 1/9000th of the flying height of the aircraft carrying the camera system.

3.4. DEM Resampling and Volume Calculation

Within the first stage of the study, using the original measurement data that were obtained with LIDAR, a numerical terrain model in the TIN format was developed. The spatial area of the polder was defined by intersecting the numerical model of the terrain with a plane to which an ordinate of the embankment spillway threshold was assigned at 94.4 m a.s.l. In this manner, a numerical LIDAR-DEM polder model was created, which was then used as the reference model. Because the spatial resolution of the ASTER-DEM, SRTM-DEM and Airborne-DEM differed and that the embankments defining the polder borders were partially or entirely left unmarked on the river side, it was assumed that all of the calculations will be carried out with the assumption that the polder border was delimited based on the LIDAR-DEM.

After the polder volume was calculated, cross-sections for each of the applied models were created to determine how the natural and artificial landscape elements are reflected, that is, slopes and river valley beds, oxbows, channels and ditches, and embankments (Figure 4).

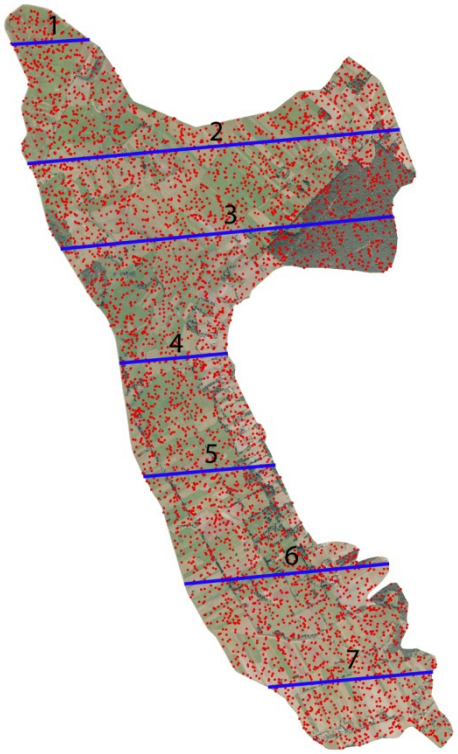

Figure 4. Cross-section of the polder and location of the points that were used to estimate the mean square error (RMSE).

4. Results

The evaluation of the influence of spatial resolution on the result of the polder volume calculations was carried out with the LIDAR-DEM model at spatial resolution of 1 m. For the LIDAR-DEM and Airborne-DEM, polder models were created at spatial resolutions of 5, 10, 25, 50, 50 and 100 m. Thereafter, the polder volume and flood zone were calculated for each model. The change in spatial resolution was carried out by the calculation of mean height within unit area (model pixel). The applied resampling method allowed the simulation of the sensor operating at a varying spatial resolution [60].

In parallel, while calculating the polder volume with the LIDAR-DEM and heights recorded in 5000 random points (Figure 4), the RMSE was calculated (Table 3) as follows:

$$\mathrm{RMSE} = \sqrt{\frac{\sum_{i=1}^{n} \left(z_{model} - z_{LiDAR-DEM}\right)^2}{n}}$$

where z_{model} means the height of the given model, and $z_{LIDAR\text{-}DEM}$ means the height of the reference terrain model form of the DEM that was developed based on the LIDAR data.

Table 3. RMSE for DEM models.

	Airborne-DEM	ASTER-DEM	SRTM-DEM
RMSE	0.657	3.973	5.399

The impact of the reduced LIDAR-DEM and Airborne-DEM resolution (resampling spatial resolutions from 1 m to 5, 10, 25, 50 and 100 m) on the determination of the polder volume was analyzed (Figures 5 and 6). In the case of the DEM based on LIDAR, resampling changed the determined volume by approximately 890,585 m^3 (difference between 1 and 100 m spatial resolution), which corresponds to approximately 10.7% of the volume as determined for the LIDAR-DEM (resolution 1 m). *Horritt et al.* and Cotter *et al.* have also obtained similar results in their studies with a resolution of 100 m and higher [61,62]. In the case of the Airborne-DEM, the maximum difference amounted to 1,119,948 m^3, which is approx. 9.5% (resolution 1 m). Changes in the range of about 10% depending on the spatial resolution demonstrate little impact on the resolution of the results obtained. Therefore, a direct comparison of the models LIDAR, SRTM and ASTER is possible.

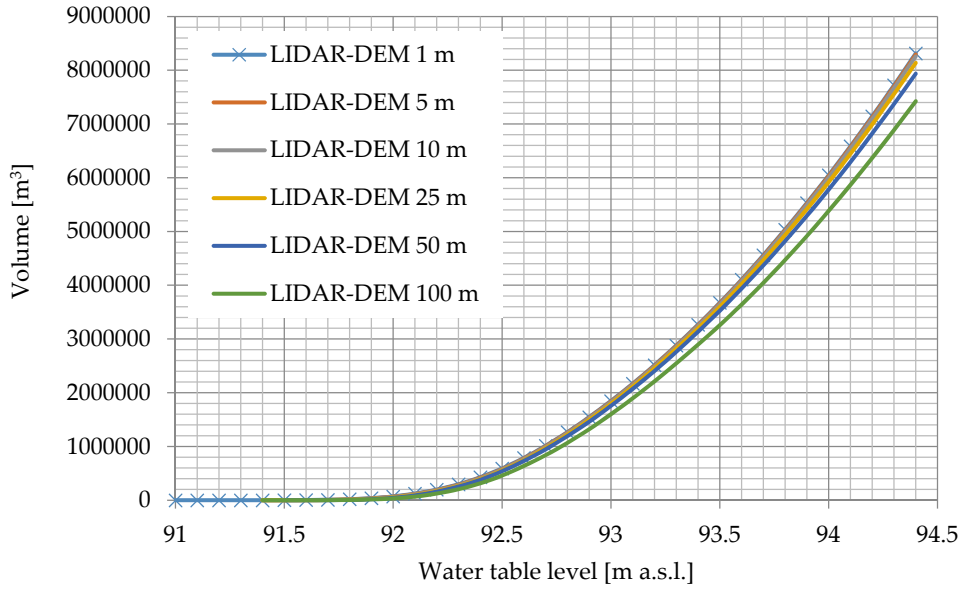

Figure 5. Comparison of the polder volume depending on the resolution of the LIDAR-DEM.

In addition, for the LIDAR-DEM, Airborne-DEM, ASTER-DEM and SRTM-DEM polder models, volume and area curves were developed to reflect the correlation of altitude against the volume and area below the defined ordinate. The calculations were performed between 90.3 m a.s.l. and 94.4 m a.s.l. at a gradation of 0.1 m (Figures 7 and 8).

The determined polder volume for ordinate 93.4 (Powiercie spillway threshold ordinate) was 3,265,611 m^3 in the case of the LIDAR-DEM, while for the Airborne-DEM it was 6,145,217 m^3, which is twice as high. In the case of the ASTER-DEM and SRTM-DEM, the calculated volumes are even

higher, reaching 16,708,307 m^3 for ASTER (5 times higher) and 23,760,684 m^3 for SRTM (more than 7 times higher). Having considered the adjustment of systematic error for the SRTM-DEM, the estimated polder volume amounted to 8,601,406 m^3 (approximately three times higher than LIDAR). The great differences between the calculated areas are visible particularly for low water levels ordinates between 91.5 and 93.0 m a.s.l. For the ordinate of 93.4 m a.s.l., the difference between the LIDAR-DEM and Airborne-DEM was 781,421 m^2. The Airborne-DEM model indicates a larger flood zone area. In addition, the flood zones that were obtained with the specific models were analyzed (Figure 9a–e). According to the analysis of the flood zones depending on the applied DEM, the zone that resembled the reference model the most was recorded in the DEM Airborne-DEM and second in the ASTER-DEM. Without the altitude correction, the SRTM-DEM may only reflect the estimated flood zone, with numerous 'isles' that indicate flood-safe spots. The adjustment correction greatly improves the entire image, however, there are still quite significant differences compared to the LIDAR-DEM (Figure 10a–f).

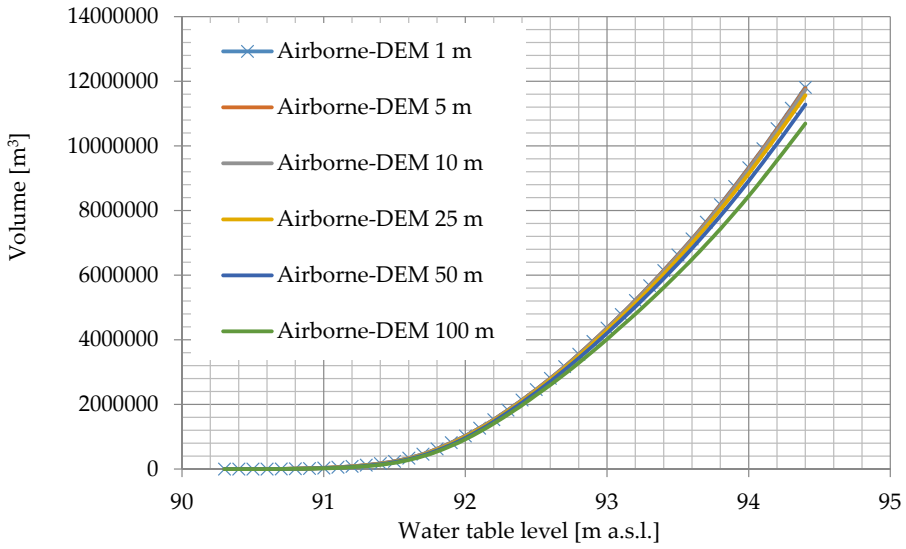

Figure 6. Comparison of the polder volume depending on the resolution of the Airborne-DEM.

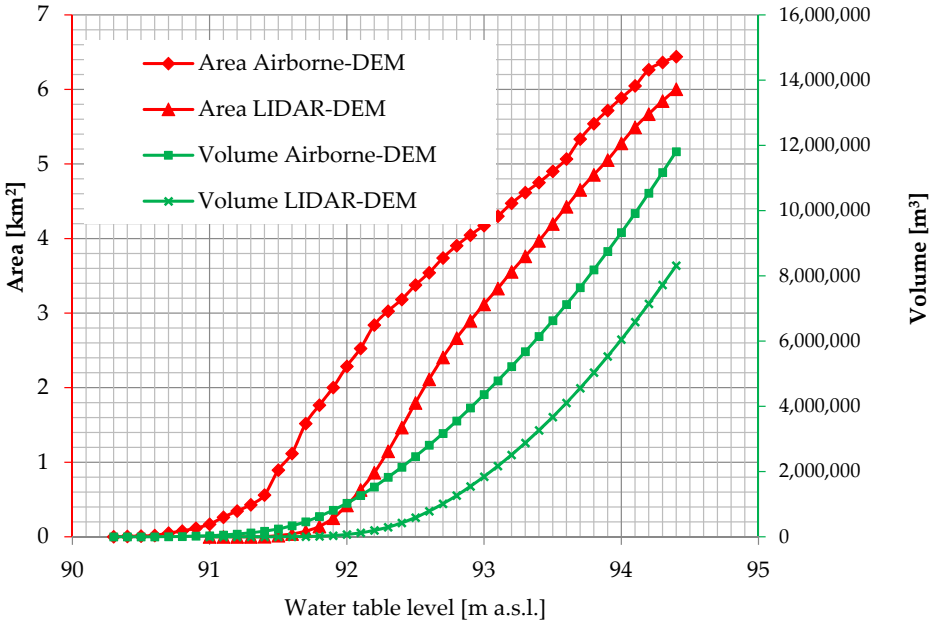

Figure 7. The volume and surface area based on the polder water table altitude.

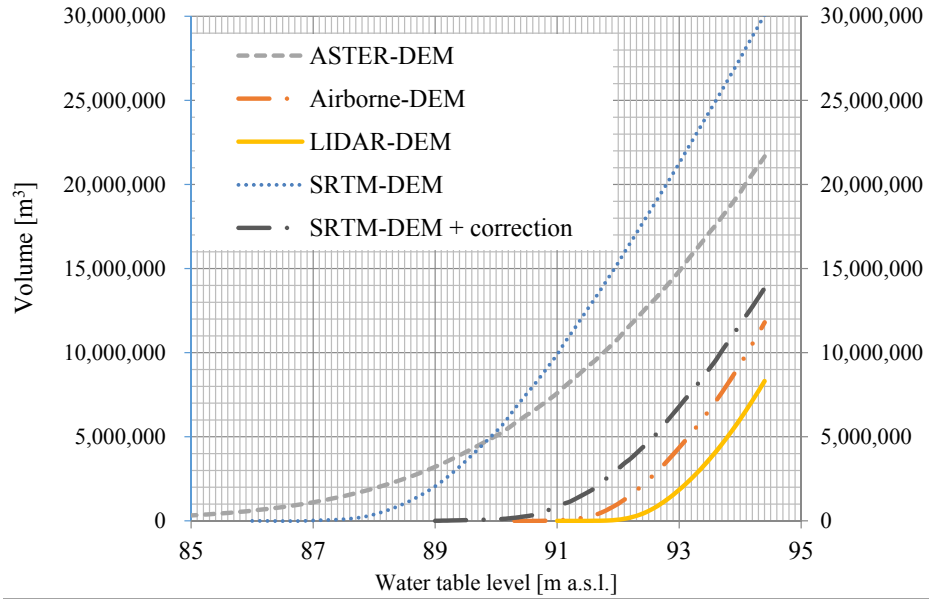

Figure 8. Comparison of the volume of the polder as determined for different DEMs.

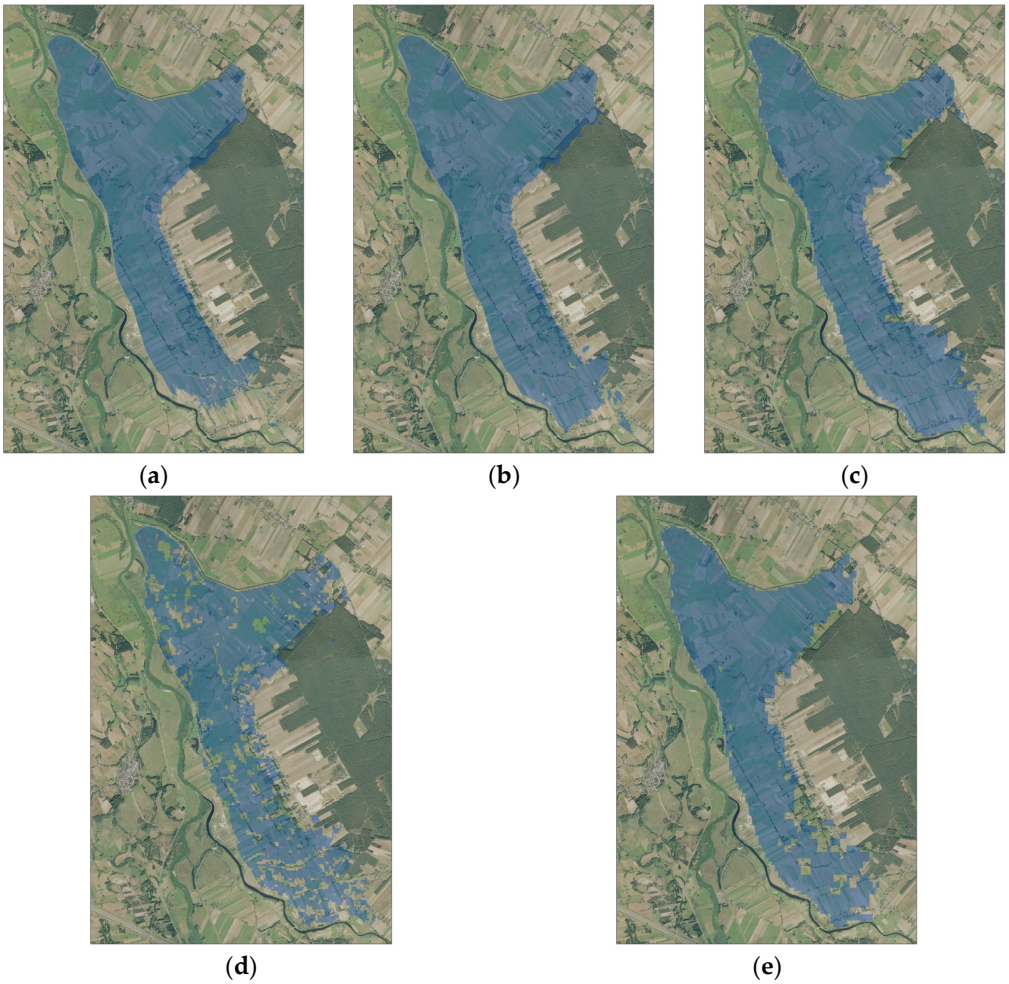

Figure 9. Flood zone of the specific DEMs (LIDAR, Airborne, ASTER, SRTM and SRTM_cor) for the maximum ordinate of 94.4 m a.s.l., (**a**) LIDAR-DEM; (**b**) Airborne-DEM; (**c**) ASTER-DEM; (**d**) SRTM-DEM; (**e**) SRTM-DEM + correction 2.67 m.

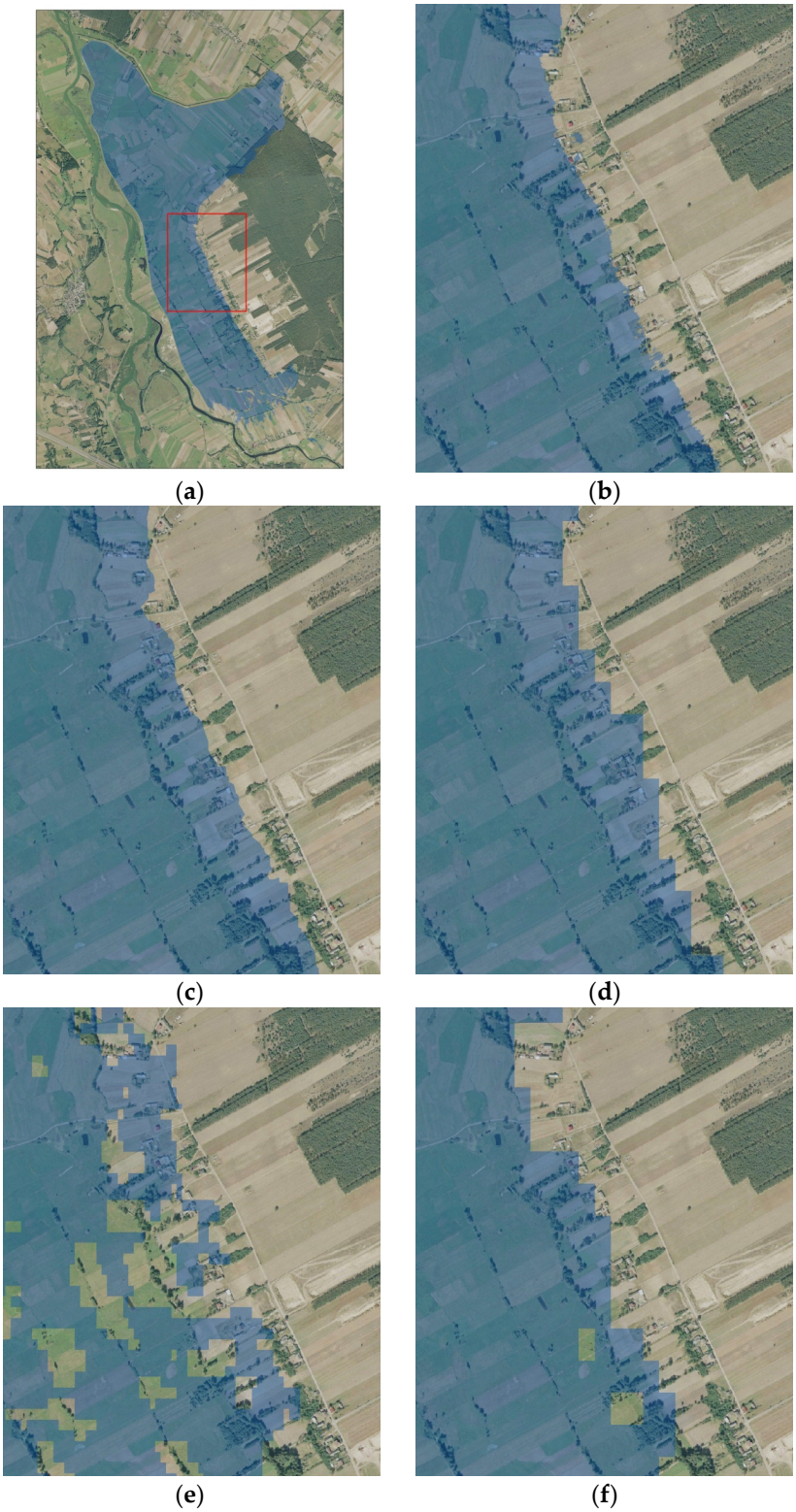

Figure 10. Flood zones in the Majdany area as defined with LIDAR, Airborne, ASTER, SRTM and SRTM_cor, (**a**) Polder, red area—Majdany village in magnification in the figure **b**–**f**; (**b**) LIDAR-DEM; (**c**) Airborne-DEM; (**d**) ASTER-DEM; (**e**) SRTM-DEM; (**f**) SRTM_cor-DEM.

Figure 11 presents a comparison of a few selected polder cross-sections that were generated for various DEMs.

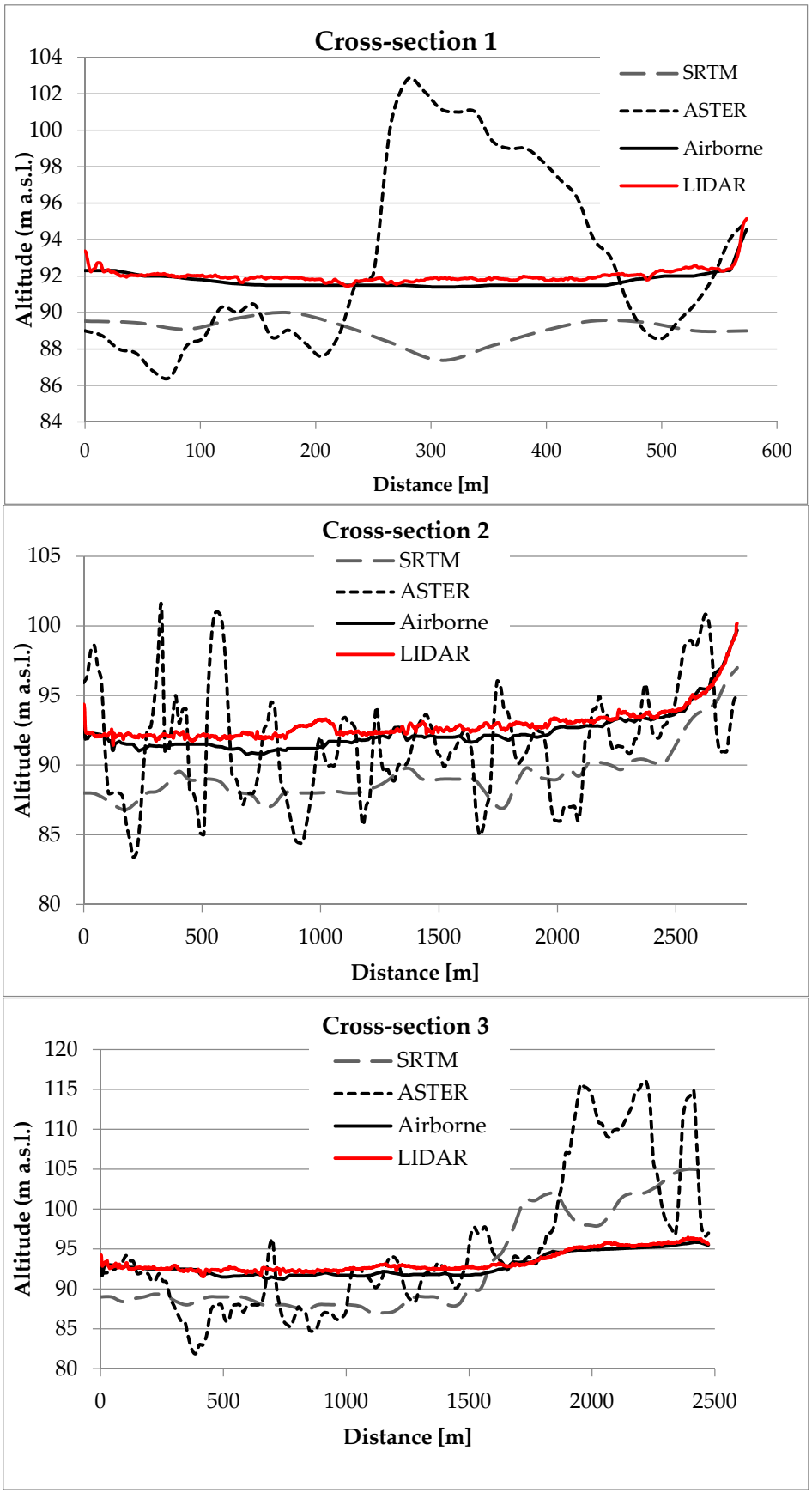

Figure 11. *Cont.*

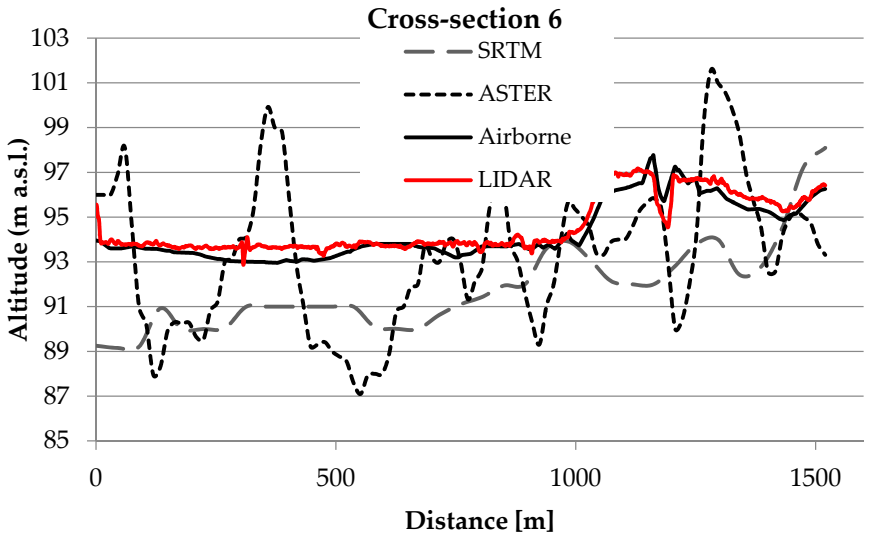

Figure 11. Comparison of cross-sections through the polder for different models of DEM.

There is a high correlation between the generated profiles and the data that were provided with the Airborne-DEM and LIDAR-DEM. The profiles that were developed for the ASTER-DEM and SRTM-DEM diverge significantly from the LIDAR-DEM. This trend is also evident from the correlations between the specific models and the reference model for 5000 random points (Figure 12). By analyzing the data that were obtained from the SRTM model, a systematic error of 2.67 m was detected. Thus, the SRTM-DEM was duly corrected by creating the SRTM_cor. However, it is worth noting that the estimate of the systematic error was possible only owing to the fact that extensive records of geodetic GPS measurement data were collected. In practice, such verification is not always possible, and the data are narrowed only to the necessary measurements, e.g., the hydrotechnical infrastructure and its vicinity.

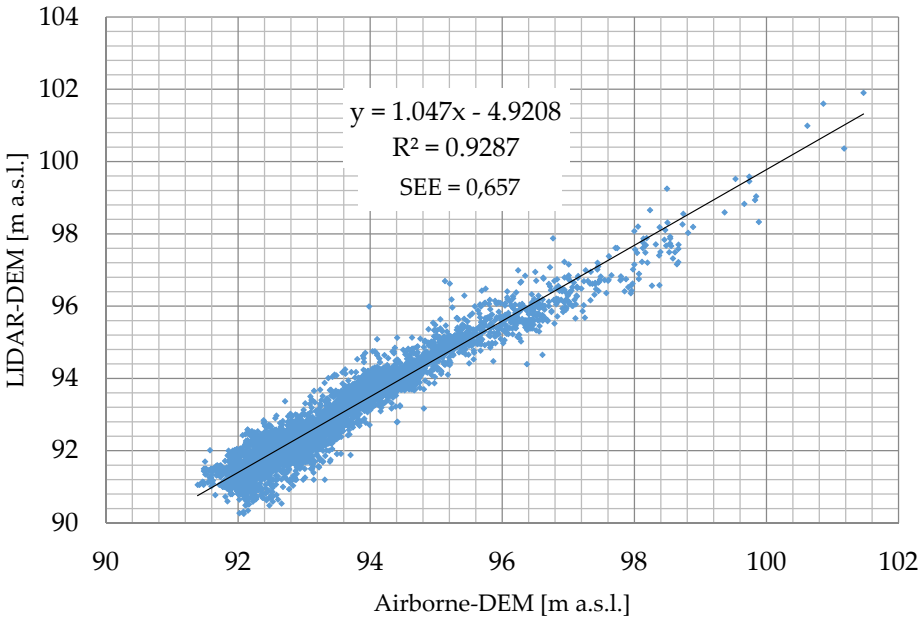

Figure 12. *Cont.*

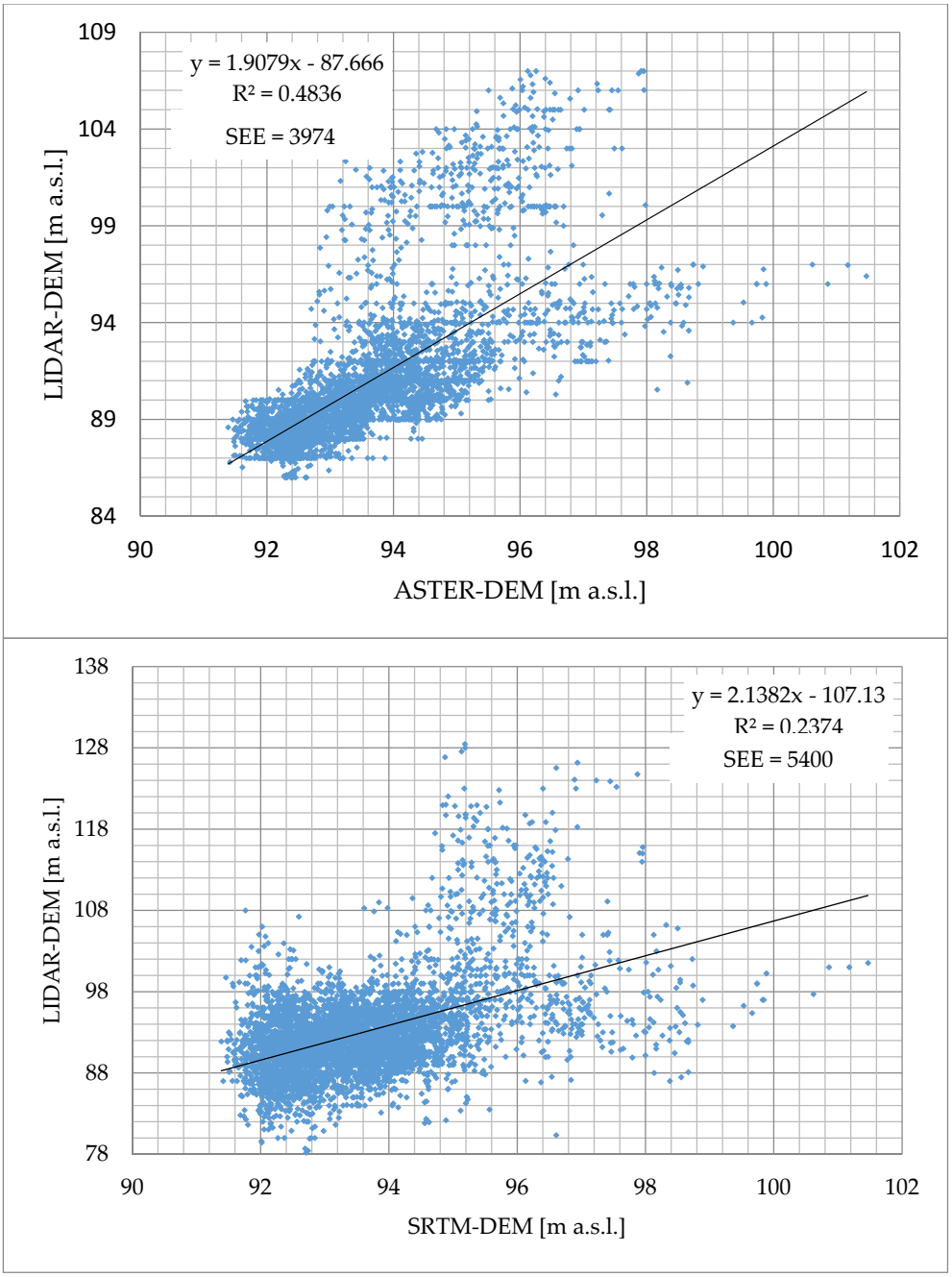

Figure 12. Comparison of the correlation between the specific models (TIN, ASTER and SRTM) and the reference model.

A high correlation was only recorded in the case of the Airborne-DEM (R^2 = 0.9287). Regarding the ASTER-DEM, the correlation amounted only to 0.4836, whereas in the SRTM-DEM, the correlation is non-existent (R^2 = 0.2374). This result indicates the low usability of free DEMs ASTER and SRTM for modeling the polder volume and operation.

5. Discussion

Digital Elevation Models play an important role in terrain analysis, and their accuracy and resolution is crucial for hydrological and hydrodynamic models. The accuracy and resolution of the DEMs have serious implications on modeling of natural processes [32]. Significant advances in

remote sensing technology have led to higher quality DEMs being generated by different techniques (contour-derived, photogrammetric, LIDAR- and RADAR-DEMs) [63]. Thomas *et al.* [63] and Schumann *et al.* [15] indicated that SRTM and ASTER elevation datasets provide equally reliable representation, hence a valid source of topographic information, and are useful in a large scale. In a smaller scale, as indicated in this paper, the ASTER and SRTM digital elevation models were not considered viable volume sources due to large deviations from the reference data. Mondal *et al.* [64] concluded that DEMs with higher accuracy (LiDAR DEMs, planimetric survey DEMs, aerial photo DEMs) will give more accurate results and will reduce the uncertainty.

Based on the results obtained in this study, the RMSE for Airborn-DEMs has a range of up $\pm$0.657 m, while ME = 0.51 m are comparable to those obtained by Wang at all [65]. Pulighe and Fava [66] reported that obtained accuracy (RMSE of $\pm$4.9 m) for DEMs based on archive aerial photos are higher than Aster (RMSE = $\pm$12.95 m) for their study area. The basic statistics of errors in ASTER-DEM show a mean error of 2.7 m and vertical accuracy RMSE 3.97 m. In the SRTM-DEM, mean error is in the 0.59 m level and RSME accuracy 5.39 m. The RSME shows that in this case the ASTER-DEM have a better vertical accuracy than the SRTM-DEM. Similar results in relation to DEMs obtained by Mukherjee *et al.* [67] where the ASTER-DEMs have better accuracy (RMSE = 6.08 m) than the SRTM (RMSE = 9.2 m). The large variation in RMSE (see Table 4) seems to be consistent with that found in other research.

Table 4. Varying reported height accuracies for the ASTER-GDEM2 and SRTM-DEMs based on [57] and other publications (unit in meters).

Studies	Study Areas	ASTER-GDEM2		SRTM v4.1	
		ME	RMSE	ME	RMSE
Suwandana *et al.* [68]	Karian Dam, Indonesia	N/A	5.68	N/A	3.25
Rexer and Hirt [69]	Australia (Bare areas)	−4.22	8.05	2.69	3.43
Li *et al.* [70]	China (Tibetan Plateau)	−5.9	14.1	0.9	8.6
Mukherjee *et al.* [67]	Shiwalik Himalaya, India	−2.58	6.08	−2.94	9.2
Athmania and Achour [57]	Anaguid test site	−2.32	5.3	0.48	3.6
	Tebessa test site	−1.02	9.8	0.48	8.3
Pulighe and Fava [66]	Italy, southern Sardinia	5.82	12.95	N/A	N/A
Wang, *et al.* [71]	Southeast Tibet		15.4		13.5
Forkuor and Maathuis [54]	Ghana Guinea Savannah	−3.30	5.46	3.67	4.95
	Ghana Volta Lake	−3.32	18.76	2.09	14.54
This study	Majadny polder	2.7	3.97	0.61	5.39

High compliance with the reference model LIDAR-DEM occurred only for the Airborne-DEM model (R^2 = 0.93). For the ASTER-DEM model, coefficient R^2 was only 0.48, while for the SRTM-DEM model only 0.24. This indicates an inadequate usefulness of generally available, free-of-charge DEMs (ASTER and SRTM) for capacity and hydrodynamic modeling of a polder. However, in other studies [54,57,70] correlations R^2 for elevation are above 0.9 for large areas. Depending on region [55], there is no obvious relationship between the DEM-GCP (Ground Control Points) differences and actual elevation for either ASTER or the reference DEMs. The differences between the reference model and ASTER-, SRTM-DEM elevation may be in the range of up to 120 m [55]. In this study, the differences are varied but maximum differences between LIDAR-DEM and Airborne-, ASTER- and SRTM-DEMs are 4.13, 18.6 and 49.55 m respectively, which can be observed in Figures 9 and 10.

The advantage of LiDAR-DEM in relation to the free-of-charge DEMs is its accuracy and resolution. In many countries, LiDAR-DEMs developed on data from one measurement are available, which will not allow analysis of the temporal changes. The LiDAR data storage requirement and DEM processing times will be higher than in other methods. Strategies for handling the large volumes of terrain data without sacrificing accuracy are required [72].

Grohmann and Sawakuchi [35] indicated that cell size of LiDAR-DEM have an impact on calculated volume. This can be explained by a random factor among the size of the cell, the size of the landforms and the position of the cell with reference to the landforms, where a small change

in cell size can lead to an under- or overestimation of the volume. Zandbergen [73] indicates that DEM cell resolution has a very strong effect on the occurrence of depressions. Otherwise, Tan *et al.* [74] indicate that DEM resolution is the most sensitive parameter compared to the DEM source and DEM resampling technique for simulating the hydrological processes. Changes in volume of the polder in the range of 10%, depending on the LIDAR-DEM resolution, indicate the small impact of this parameter on the results obtained in this study. It means it is possible, in this case, to reduce sample data to create DEMs.

Polder volume estimated at the stage of the project [75] was 3,700,000 m^3. The actual volume, based on LIDAR data is lower by about 22% (3,265,611 m^3). This is confirmed by the results obtained in the project [30]. Volume estimated based on other DEM models are twice (Airborne-DEM) and up to seven times higher (SRTM-DEM) than the reference model. This may affect adversely the management of the flood system. Low accuracy of ASTER and SRTM data in this particular application makes it impossible to use them for hydrological modeling.

6. Conclusions

The four digital elevation models (LiDAR-, Airborne-, ASTER- and SRTM-DEM) were tested to define polder retention capacities. The LiDAR-DEM supported by our GCPs measurements was used as a reference model. Because the spatial resolutions of all DEMs are different, the spatial resolution of the LiDAR-DEM and Airborne-DEM on the calculated polder volume was evaluated. Changes in volume of the polder range of 10%, depending on the DEMs resolution in topographically homogeneous floodplains, indicate the small impact of this parameter on the results obtained in this study. It is possible, therefore, to make a direct comparison of the models LIDAR, SRTM and ASTER.

Free and generally available ASTER or SRTM DEMs allow for the quick development of terrain models. However, the accuracy of these models (mean error of 2.7 m and 0.59 m and vertical accuracy RMSE 3.97 m and 5.39 m for ASTER-DEM and SRTM-DEM, respectively) is insufficient for modeling the transformation of flood waves, modeling polders as flood-protection systems, and defining flood zones. High correlation (R^2 = 0.9287) was recorded only between the LiDAR and Airborne data. Free-of-charge DEMs characterized a small correlation (0.48 and 0.24 for ASTER and SRTM, respectively) and this indicates low usability for modeling the polder volume and operation. The polder volume, estimated at the reference model (LiDAR-DEM), is 3.2 million m^3. Estimated volume based on the ASTER-DEM was five times higher, and seven times for the SRTM-DEM. The low accuracy of ASTER and SRTM data in this particular application make them unviable for use in hydrological modeling.

The model and data quality improvement procedures that were used in SRTM, by means of defining the systematic error and the appropriate adjustment offset, are to some extent effective but still insufficient for river flow modeling or the delimitation of flood zones. These procedures also require a large number of field measurements (e.g., based on geodetic GPS measurements) to specify the necessary adjustments.

The LiDAR-DEMs provide the most accurate information about terrain and should be treated as a reference for hydrodynamic modeling. In the absence of the availability of LIDAR-DEMs, Airborne-DEMs can be used in hydrodynamic modeling. However, these models must also be tested and corrected on the basis of field measurements.

The vertical accuracy of available ASTER- and SRTM-DEMs is insufficient to calculate the polder volume and model the transformation of flood waves in river systems. The spatial accuracy of the ASTER and SRTM models is insufficient due to their lack of good reproduction of levee embankments in order to determine the polder boundary. These models may, however, become useful for certain cartographic studies.

Acknowledgments: This study was financially supported by Polish Ministry of Science and Higher Education (Project No. N N523 744940) in terms of field measurements and data acquisition, Institute of Construction and Geoengineering, Department of Land Improvement, Environmental Development and Geodesy and Faculty

of Environmental Engineering and Land Management in terms of publication fees. We thank the editor and reviewers for their professional comments and corrections.

Author Contributions: Zbigniew Walczak contributed in data collection, prepared discussion and conclusions, prepared graphs for final presentation of results, made text formatting for final publication. Rafał Wróżyński contributed in data collection and analysis, preparation of data for simulations. Mariusz Sojka was responsible for statistical analysis of collected data, preparation of graphs and maps for final presentation of results, contributed discussion and conclusions. Ireneusz Laks contributed in data collection.

Conflicts of Interest: The authors declare no conflict of interest.

References

1. Banasiak, R. Use of GIS technics and numerical hydrodynamic models for flood hazard assessment. *Infrastrukt. I Ekol. Teren. Wiej.* **2012**, *3*, 123–134. (In Polish)
2. Teng, J.; Vaze, J.; Dutta, D.; Marvanek, S. Rapid Inundation Modelling in Large Floodplains Using LiDAR DEM. *Water Resour. Manag.* **2015**, *29*, 2619–2636. [CrossRef]
3. Costabile, P.; Macchione, F.; Natale, L.; Petaccia, G. Flood mapping using LIDAR DEM. Limitations of the 1-D modeling highlighted by the 2-D approach. *Nat. Hazards* **2015**, *77*, 181–204. [CrossRef]
4. Schellekens, J.; Brolsma, R.J.; Dahm, R.J.; Donchyts, G.V.; Winsemius, H.C. Rapid setup of hydrological and hydraulic models using OpenStreetMap and the SRTM derived digital elevation model. *Environ. Model. Softw.* **2014**, *61*, 98–105. [CrossRef]
5. Sanecki, J.; Pabisiak, P.; Bauer, R.; Ptak, A.; Stępień, G. The application of DEM and DSM in analysis of flood areas. *Folia Sci. Univ. Tech. Resoviensis* **2012**, *59*, 287–293.
6. Bouwer, L.; Bubeck, P.; Wagtendonk, A.; Aerts, J. Inundation scenarios for flood damage evaluation in polder areas. *Nat. Hazards Earth Syst. Sci.* **2009**, *9*, 1995–2007. [CrossRef]
7. Laks, I.; Kałuża, T. Influence of Konin-Pyzdry valley and Golina polder on flow routing in the Warta river. *Zesz. Naukowe Akad. Rol. We Wroc. Inzynieria Srodowiska* **2006**, *15*, 175–183.
8. Przybyła, C.; Bykowski, J.; Mrozik, K.; Napierała, M. The role of Zagorow polder in flood protection. *Rocz. Ochr. Środowiska Sel. Full Texts* **2011**, *13*, 801–813.
9. Wit, M. Depression of the flood wave culmination by the use of the Smolice polder to protect the town Cracow againts the flood. *Gospod. Wodn.* **1999**, *3*, 98–100. (In Polish)
10. Laks, I.; Kałuża, T.; Sojka, M.; Walczak, Z.; Wróżyński, R. Problems with modelling water distribution in open channels with hydraulic engineering structures. *Annu. Set Environ. Prot.* **2013**, *15*, 245–257.
11. Kowalik, P. Flood control in the Vistula river delta (Poland). *Environ. Biotechnol.* **2008**, *4*, 1–6.
12. Gichamo, T.Z.; Popescu, I.; Jonoski, A.; Solomatine, D. River cross-section extraction from the ASTER global DEM for flood modeling. *Environ. Model. Softw.* **2012**, *31*, 37–46. [CrossRef]
13. Tarekegn, T.H.; Haile, A.T.; Rientjes, T.; Reggiani, P.; Alkema, D. Assessment of an ASTER-generated DEM for 2D hydrodynamic flood modeling. *Int. J. Appl. Earth Obs. Geoinform.* **2010**, *12*, 457–465. [CrossRef]
14. Forkuo, E.K. Flood hazard mapping using Aster image data with GIS. *Int. J. Geomat. Geosci.* **2011**, *1*, 932–950.
15. Schumann, G.; Matgen, P.; Cutler, M.E.J.; Black, A.; Hoffmann, L.; Pfister, L. Comparison of remotely sensed water stages from LiDAR, topographic contours and SRTM. *ISPRS J. Photogramm. Remote Sens.* **2008**, *63*, 283–296. [CrossRef]
16. Ludwig, R.; Schneider, P. Validation of digital elevation models from SRTM X-SAR for applications in hydrologic modeling. *ISPRS J. Photogramm. Remote Sens.* **2006**, *60*, 339–358. [CrossRef]
17. Patro, S.; Chatterjee, C.; Mohanty, S.; Singh, R.; Raghuwanshi, N. Flood inundation modeling using MIKE FLOOD and remote sensing data. *J. Indian Soc. Remote Sens.* **2009**, *37*, 107–118. [CrossRef]
18. Hejmanowska, B. Influence of data quality on modeling of flood zones. *Pol. Ttowarzystwo Inf. Przestrz. Rocz. Gematyki* **2006**, *IV*, 145–152.
19. Hejmanowska, B. NMT (GRID/TIN) analysis-Oki data example. *Arch. Fotografi-Metrii Kartogr. I Teledetekcji* **2007**, *17*, 281–289.
20. Hejmanowska, B.; Drzewiecki, W.; Kulesza, Ł. The quality of digital terrain models. *Arch. Fotogram. Kartogr. I Teledetekcji* **2008**, *18*, 163–176.
21. Wang, X.; Lin, Q. Effect of DEM mesh size on AnnAGNPS simulation and slope correction. *Environ. Monit. Assess.* **2011**, *179*, 267–277. [CrossRef] [PubMed]

22. Cook, A.; Merwade, V. Effect of topographic data, geometric configuration and modeling approach on flood inundation mapping. *J. Hydrol.* **2009**, *377*, 131–142. [CrossRef]
23. Pramanik, N.; Panda, R.; Sen, D. One Dimensional Hydrodynamic Modeling of River Flow Using DEM Extracted River Cross-sections. *Water Resour. Manag.* **2010**, *24*, 835–852. [CrossRef]
24. Zhao, Z.; Benoy, G.; Chow, T.; Rees, H.; Daigle, J.-L.; Meng, F.-R. Impacts of Accuracy and Resolution of Conventional and LiDAR Based DEMs on Parameters Used in Hydrologic Modeling. *Water Resour. Manag.* **2010**, *24*, 1363–1380. [CrossRef]
25. Walczak, Z.; Sojka, M.; Laks, I. Assessment of mapping of embankments and control structure on digital elevation model based up on Majdany polder. *Ann. Set Environ. Prot.* **2013**, *15*, 2711–2724.
26. Merwade, V.; Cook, A.; Coonrod, J. GIS techniques for creating river terrain models for hydrodynamic modeling and flood inundation mapping. *Environ. Model. Softw.* **2008**, *23*, 1300–1311. [CrossRef]
27. Liro, A. *Strategia Wdrażania Krajowej Sieci Ekologicznej ECONET-Polska*; Fundacja IUCN: Warszawa, Poland, 1998.
28. BirdLife.org. Avaliable online: http://www.birdlife.org/datazone/sitefactsheet.php?id=926 (accessed on 25 May 2016).
29. Rozporządzenie Ministra Ochrony Środowiska, Zasobów Naturalnych i Leśnictwa z dnia 20 kwietnia 2007 r. w sprawie warunków technicznych, jakim powinny odpowiadać obiekty budowlane gospodarki wodnej i ich usytuowanie. Dz.U. 2007 nr 86 poz. 579. 2007.
30. ISOK. IT system of the Country's Protection Against Extreme Harazds (ISOK). Avaliable online: http://www.isok.gov.pl/en/ (accessed on 25 May 2016).
31. Hladik, C.; Alber, M. Accuracy assessment and correction of a LIDAR-derived salt marsh digital elevation model. *Remote Sens. Environ.* **2012**, *121*, 224–235. [CrossRef]
32. Vaze, J.; Teng, J.; Spencer, G. Impact of DEM accuracy and resolution on topographic indices. *Environ. Model. Softw.* **2010**, *25*, 1086–1098. [CrossRef]
33. Hodgson, M.E.; Bresnahan, P. Accuracy of airborne lidar-derived elevation: Empirical assessment and error budget. *Photogramm. Eng. Remote Sens.* **2004**, *70*, 331–340. [CrossRef]
34. Liu, X. Airborne LiDAR for DEM generation: Some critical issues. *Prog. Phys. Geogr.* **2008**, *32*, 31–49.
35. Grohmann, C.H.; Sawakuchi, A.O. Influence of cell size on volume calculation using digital terrain models: A case of coastal dune fields. *Geomorphology* **2013**, *180–181*, 130–136. [CrossRef]
36. Anderson, E.S.; Thompson, J.A.; Crouse, D.A.; Austin, R.E. Horizontal resolution and data density effects on remotely sensed LIDAR-based DEM. *Geoderma* **2006**, *132*, 406–415. [CrossRef]
37. Zhang, K.; Chen, S.-C.; Whitman, D.; Shyu, M.-L.; Yan, J.; Zhang, C. A progressive morphological filter for removing nonground measurements from airborne LIDAR data. *Geosci. Remote Sens.* **2003**, *41*, 872–882. [CrossRef]
38. Cobby, D.M.; Mason, D.C.; Davenport, I.J. Image processing of airborne scanning laser altimetry data for improved river flood modelling. *ISPRS J. Photogramm. Remote Sens.* **2001**, *56*, 121–138. [CrossRef]
39. Meng, X.; Currit, N.; Zhao, K. Ground filtering algorithms for airborne LiDAR data: A review of critical issues. *Remote Sens.* **2010**, *2*, 833–860. [CrossRef]
40. Zhang, K.; Whitman, D. Comparison of three algorithms for filtering airborne lidar data. *Photogramm. Eng. Remote Sens.* **2005**, *71*, 313–324. [CrossRef]
41. Farr, T.G.; Rosen, P.A.; Caro, E.; Crippen, R.; Duren, R.; Hensley, S.; Kobrick, M.; Paller, M.; Rodriguez, E.; Roth, L. The shuttle radar topography mission. *Rev. Geophys.* **2007**, *45*. [CrossRef]
42. Rodriguez, E.; Morris, C.S.; Belz, J.E. A global assessment of the SRTM performance. *Photogramm. Eng. Remote Sens.* **2006**, *72*, 249–260. [CrossRef]
43. Karwel, A.K.; Ewiak, I. Estimation of the accuracy of the SRTM terrain model in Poland. *Arch. Fotogram. Kartogr. I Teledetekcji* **2006**, *16*, 289–296. (In Polish) [CrossRef]
44. Karwel, A.K.; Ewiak, I. Assessment of useufulness of SRTM data for generation of DEM of the territory of Poland. *Pr. Inst. Geod. I Kartogr.* **2006**, *52*, 75–87. (In Polish)
45. Hofton, M.; Dubayah, R.; Blair, J.B.; Rabine, D. Validation of SRTM elevations over vegetated and non-vegetated terrain using medium footprint lidar. *Photogramm. Eng. Remote Sens.* **2006**, *72*, 279–285. [CrossRef]
46. Jarvis, A.; Rubiano, J.; Nelson, A.; Farrow, A.; Mulligan, M. Practical use of SRTM data in the tropics: Comparisons with digital elevation models generated from cartographic data. *Work. Doc.* **2004**, *198*, 32.

47. Abrams, M. The Advanced Spaceborne Thermal Emission and Reflection Radiometer (ASTER): Data products for the high spatial resolution imager on NASA's Terra platform. *Int. J. Remote Sens.* **2000**, *21*, 847–859. [CrossRef]
48. Cuartero, A.; Felicísimo, A.; Ariza, F. Accuracy of DEM generation from Terra-Aster stereo data. *Int. Arch. Photogramm. Remote Sens.* **2004**, *35*, 559–563.
49. Hirano, A.; Welch, R.; Lang, H. Mapping from ASTER stereo image data: DEM validation and accuracy assessment. *ISPRS J. Photogramm. Remote Sens.* **2003**, *57*, 356–370. [CrossRef]
50. Yamaguchi, Y.; Kahle, A.B.; Tsu, H.; Kawakami, T.; Pniel, M. Overview of advanced spaceborne thermal emission and reflection radiometer (ASTER). *Geosci. Remote Sens.* **1998**, *36*, 1062–1071. [CrossRef]
51. Lewiński, S.; Ewiak, I. Preliminary assessment of usefulness of ASTER satellite images in remote sensing and photogrammetry. *Arch. Fotogra. Kartogr. I Teledetekcji* **2004**, *14*, 369–380. (In Polish)
52. Przybyła, C.; Pyszny, K. Comparison of Digital Elevation Models SRTM and ASTER GDEM and evaluation of the possibility of their use in hydrological modeling in areas of low drop. *Ann. Set Environ. Prot.* **2013**, *15*, 1489–1510.
53. Nikolakopoulos, K.G.; Kamaratakis, E.K.; Chrysoulakis, N. SRTM *vs.* ASTER elevation products. Comparison for two regions in Crete, Greece. *Int. J. Remote Sens.* **2006**, *27*, 4819–4838. [CrossRef]
54. Forkuor, G.; Maathuis, B. Comparison of SRTM and ASTER Derived Digital Elevation Models over Two Regions in Ghana–Implications for Hydrological and Environmental Modeling. *Stud. Environ. Appl. Geomorphol.* **2012**, 219–240. [CrossRef]
55. Slater, J.A.; Heady, B.; Kroenung, G.; Curtis, W.; Haase, J.; Hoegemann, D.; Shockley, C.; Tracy, K. *Evaluation of the New ASTER Global Digital Elevation Model*; National Geospatial-Intelligence Agency: Springfield, VA, USA, 2009. Avaliable online: http://earth-info.nga.mil/GandG/elevation/ (accessed on 25 May 2016).
56. Huggel, C.; Schneider, D.; Miranda, P.J.; Delgado Granados, H.; Kääb, A. Evaluation of ASTER and SRTM DEM data for lahar modeling: A case study on lahars from Popocatépetl Volcano, Mexico. *J. Volcanol. Geotherm. Res.* **2008**, *170*, 99–110. [CrossRef]
57. Athmania, D.; Achour, H. External validation of the ASTER GDEM2, GMTED2010 and CGIAR-CSI-SRTM v4. 1 free access digital elevation models (DEMs) in Tunisia and Algeria. *Remote Sens.* **2014**, *6*, 4600–4620. [CrossRef]
58. Kääb, A. Combination of SRTM3 and repeat ASTER data for deriving alpine glacier flow velocities in the Bhutan Himalaya. *Remote Sens. Environ.* **2005**, *94*, 463–474. [CrossRef]
59. Henry, J.B.; Malet, J.P.; Maquaire, O.; Grussenmeyer, P. The use of small-format and low-altitude aerial photos for the realization of high-resolution DEMs in mountainous areas: Application to the Super-Sauze earthflow (Alpes-de-Haute-Provence, France). *Earth Surf. Proc. Land.* **2002**, *27*, 1339–1350. [CrossRef]
60. Grohmann, C.H.; Smith, M.J.; Riccomini, C. Multiscale analysis of topographic surface roughness in the Midland Valley, Scotland. *Geosci. Remote Sens.* **2011**, *49*, 1200–1213. [CrossRef]
61. Horritt, M.; Bates, P. Effects of spatial resolution on a raster based model of flood flow. *J. Hydrol.* **2001**, *253*, 239–249. [CrossRef]
62. Cotter, A.S.; Chaubey, I.; Costello, T.A.; Soerens, T.S.; Nelson, M.A. Water quality model output uncertainty as affected by spatial resolution of input data. *J. Am. Water Resour. Assoc.* **2003**, *39*, 977–986. [CrossRef]
63. Thomas, J.; Joseph, S.; Thrivikramji, K.P.; Arunkumar, K.S. Sensitivity of digital elevation models: The scenario from two tropical mountain river basins of the Western Ghats, India. *Geosci. Front.* **2014**, *5*, 893–909. [CrossRef]
64. Mondal, A.; Khare, D.; Kundu, S.; Mukherjee, S.; Mukhopadhyay, A.; Mondal, S. Uncertainty of soil erosion modeling using open source high resolution and aggregated DEMs. *Geosci. Front.*. [CrossRef]
65. Wang, H.; Ellis, E. Spatial accuracy of orthorectified IKONOS imagery and historical aerial photographs across five sites in China. *Int. J. Remote Sens.* **2005**, *26*, 1893–1911. [CrossRef]
66. Pulighe, G.; Fava, F. DEM extraction from archive aerial photos: Accuracy assessment in areas of complex topography. *Eur. J. Remote Sens.* **2013**, *46*, 363–378. [CrossRef]
67. Mukherjee, S.; Joshi, P.; Mukherjee, S.; Ghosh, A.; Garg, R.; Mukhopadhyay, A. Evaluation of vertical accuracy of open source Digital Elevation Model (DEM). *Int. J. Appl. Earth Obs. Geoinform.* **2013**, *21*, 205–217. [CrossRef]

68. Suwandana, E.; Kawamura, K.; Sakuno, Y.; Kustiyanto, E.; Raharjo, B. Evaluation of ASTER GDEM2 in Comparison with GDEM1, SRTM DEM and Topographic-Map-Derived DEM Using Inundation Area Analysis and RTK-dGPS Data. *Remote Sens.* **2012**, *4*, 2419. [CrossRef]
69. Rexer, M.; Hirt, C. Comparison of free high resolution digital elevation data sets (ASTER GDEM2, SRTM v2. 1/v4. 1) and validation against accurate heights from the Australian National Gravity Database. *Aust. J. Earth Sci.* **2014**, *61*, 213–226. [CrossRef]
70. Li, P.; Shi, C.; Li, Z.; Muller, J.-P.; Drummond, J.; Li, X.; Li, T.; Li, Y.; Liu, J. Evaluation of ASTER GDEM using GPS benchmarks and SRTM in China. *Int. J. Remote Sens.* **2013**, *34*, 1744–1771. [CrossRef]
71. Wang, W.; Yang, X.; Yao, T. Evaluation of ASTER GDEM and SRTM and their suitability in hydraulic modelling of a glacial lake outburst flood in southeast Tibet. *Hydrol. Process.* **2012**, *26*, 213–225. [CrossRef]
72. Kidner, D.B.; Smith, D.H. Advances in the data compression of digital elevation models. *Comput. Geosci.* **2003**, *29*, 985–1002. [CrossRef]
73. Zandbergen, P.A. The effect of cell resolution on depressions in digital elevation models. *Appl. GIS* **2006**, *2*, 04.01–04.35. [CrossRef]
74. Tan, M.L.; Ficklin, D.L.; Dixon, B.; Ibrahim, A.L.; Yusop, Z.; Chaplot, V. Impacts of DEM resolution, source, and resampling technique on SWAT-simulated streamflow. *Appl. Geogr.* **2015**, *63*, 357–368. [CrossRef]
75. Hydroprojekt. *Building-Executive Project of "Polder Majdan-Increasing the Ner and Warta River Right-Site Embankment in Dabie"*; Hydroprojekt Sp. z o.o.: Poznań, Poland, 2002.